Available online at www.sciencedirect.com

SCIENCE DIRECT®

Catalysis Today 93–95 (2004) 107–112

CATALYSIS TODAY

www.elsevier.com/locate/cattod

# Mitigation of fouling of skeletal copper catalysts for the gas-phase hydrogenolysis of methyl formate to methanol by addition of chromia

X. Huang, N.W. Cant, M.S. Wainwright*, L. Ma

*School of Chemical Engineering and Industrial Chemistry, The University of New South Wales, Sydney 2052, Australia*

## Abstract

The addition of chromia on skeletal copper catalysts has been investigated for the gas-phase hydrogenolysis of methyl formate to methanol by leaching a $CuAl_2$ alloy in the presence of sodium chromate. The presence of chromia greatly reduced skeletal copper catalyst deactivation although at the expense of some loss of activity if the chromia content was high. The differences in rates of deactivation were interpreted in terms of deposition of a foulant according to first-order kinetics based on parallel deactivation. Optimal residual activity was obtained by adding ca. 1.5 wt.% of chromia to skeletal copper during the process of leaching.

*Keywords:* Hydrogenolysis; Methyl formate; Methanol; Skeletal copper catalyst; $Cr_2O_3$; Deactivation kinetics

## 1. Introduction

The hydrogenolysis of natural fatty acid esters for production of fatty alcohols [1–3] has been operated in large-scale industrial processes for more than five decades, with particular interest in the hydrogenolysis of diesters to diols [4,5], used in the production of polyesters.

The use of copper-based catalysts for ester hydrogenolysis reactions is also well established [4–15]. Raney® copper catalysts have been widely investigated but significant deactivation has been observed [5]. Evans et al. [6] studied the hydrogenolysis of methyl formate in the gas phase over a variety of copper-based catalysts and reported that Raney® copper is the most active and selective catalyst for the reaction but is subject to severe and rapid deactivation. A recent study [16] showed that a skeletal copper catalyst, prepared using the Raney® method, lost most of its initial activity in 2 h at 101 kPa and 453 K and that deactivation was inhibited when chromia was deposited on the copper.

This paper examines the role of $Cr_2O_3$ in reducing deactivation of skeletal copper catalysts in methyl formate hydrogenolysis and models the deactivation kinetics according to power-law equations.

## 2. Experimental

### 2.1. Catalyst preparation

The chromia-promoted samples were prepared by the methods reported in earlier studies [16,17] using $CuAl_2$ (52.17 wt.% Al and 47.83 wt.% Cu) alloy obtained from Riverside Metal Industrial Pty. Ltd., Australia. The alloy was crushed and screened to particles of size 210–350 μm and then leached in a large excess of 6.1 M aqueous NaOH containing $Na_2CrO_4$ at concentrations from 0.001 to 0.6 M for 24 h at 273 K. The samples were stored in distilled water at ca. $-10\,^{\circ}C$ to avoid oxidation prior to activity evaluation.

### 2.2. Copper surface area determination

Catalyst compositions (Al and Cr metal) were determined by atomic absorption spectroscopy (Varian/Spectr AA-20 plus) on acid-digested samples. BET surface areas were measured by nitrogen adsorption (single point) at 77 K in a flow adsorption apparatus using 30 vol.% $N_2$ in He. Apparent copper surface areas were estimated by $N_2O$ decomposition at 363 K [18]. Details of the characterization procedures were described in a previous paper [17].

---

* Corresponding author. Tel.: +61 2 93852700; fax: +61 2 93858008.
*E-mail address:* m.wainwright@unsw.edu.au (M.S. Wainwright).

0920-5861/$ – see front matter © 2004 Elsevier B.V. All rights reserved.
doi:10.1016/j.cattod.2004.06.018

### 2.3. Catalyst activity measurement

The measurements of catalyst activities for the gas-phase hydrogenolysis reaction and accompanying deactivation studies were carried out in a continuous flow fixed bed micro-reactor operated at atmospheric pressure. A schematic of the system was shown in an earlier paper [19].

The reactor comprised a 6 mm (o.d.) stainless steel tube located in an air oven with the catalyst sample (ca. 0.1 g) packed near the centre of the tube. Gaseous methyl formate was introduced by passing carrier gas (20 $cm^3$ (STP)/min of hydrogen) through two saturators connected in series in a water bath at 288 K. Additional hydrogen was introduced to keep the molar ratio $H/C \geq 8$. Helium was also introduced as a diluent gas to obtain a constant space velocity at different partial pressures. The reactant and product streams were analysed by two on-line gas chromatographs (Shimadzu 9A) fitted with thermal conductivity detectors with separation using a Porapak Q column (3.2 m) held at 403 K for methanol and methyl formate and a CTR-1 column (Alltech Inc.) held at 323 K for carbon oxides and hydrogen. Condensable materials were removed using an ice bath prior to the CTR-1 column.

The conditions used to determine activities were: methyl formate partial pressure: 7.5 kPa, hydrogen partial pressure: 65 kPa, molar ratio: $H/C \geq 8$, $T$: 443–473 K, GHSV: ca. 150 000 $h^{-1}$ with product analysis carried out every 10 min. Due to the time taken to flush the saturator and reach adsorption equilibrium on the catalyst, the highest production of methyl formate was observed on the second or third analysis and the time zero on the plots that follow corresponds to that analysis.

## 3. Results and discussion

### 3.1. Effect of chromia on copper surface area

Table 1 shows that leaching in the presence of sodium chromate removed 93–99 wt.% of the aluminum from the alloy particles and deposited 0.4–5.1 wt.% $Cr_2O_3$ onto the skeletal copper. The effect of chromia deposition on the apparent copper surface area shows similar trends to those reported previously and can be interpreted in terms of the leaching kinetics [17,20,21]. The presence of sodium chromate hinders the rates of leaching and increases the residual $Al_2O_3$ with increasing $Cr_2O_3$ contents resulting in dramatically higher total surface areas due to the contributions from the oxides as well as smaller copper crystallites. These oxides must be present as thin layers or fine particles since their surface areas are very high on a mass basis – approximately 70 $m^2$ for 0.125 g of oxides in the case of Cu–Cr-7 (i.e. $\sim$560 $m^2$/g). Slower leaching with sodium chromate in the caustic solution resulted in higher copper surface areas than that of the chromia-free sample when the $Cr_2O_3$ content was low but higher $Cr_2O_3$ coverage reduced apparent Cu areas.

### 3.2. Catalytic activity

The hydrogenolysis of methyl formate to methanol (Eq. (1)) is highly exothermic and unfavorable at higher temperatures. The side reactions, such as decarbonylation or decomposition of methyl formate, are negligible under moderate conditions. Thermodynamic evaluation by Kim et al. [22] showed that below 500 K each mole fraction is constant since the chemical equilibrium is affected only by reaction (1):

$$CH_3OCHO\,(g) + 2H_2\,(g) \rightarrow 2CH_3OH\,(g) \qquad (1)$$

Under the conditions used here the equilibrium conversion is close to 100% [22]. The activity comparisons that follow were carried out with a maximum conversion of around 30%. Fig. 1 shows plots of the hydrogenolysis activities versus time on stream for catalysts containing various amounts of chromium oxide.

The unpromoted pure skeletal copper catalyst exhibited high activity when first brought on-line, but the rate dropped sharply as the catalyst adjusted to the operating conditions. Subsequent deactivation was slower, approaching a relatively steady state after 6 h. With chromia present, the initial activity decreased with increasing amounts of chromium oxide but the stability was improved significantly.

Table 1
Properties of un-promoted and promoted skeletal copper samples

| Skeletal catalyst[a] | Chromium solution[a] | Composition (wt.%) | | | Surface area ($m^2$/g) | | |
|---|---|---|---|---|---|---|---|
| | | Cu | $Al_2O_3$ | $Cr_2O_3$ | $S_{BET}$ | $S_{Cu}$ | $S_{Cu}/S_{BET}$ |
| Cu-A | n/a | 98.53 | 1.47 | 0.00 | 25.3 | 9.9 | 0.39 |
| Cu–Cr-1 | 0.001 M $CrO_4^{2-}$ | 97.31 | 2.30 | 0.39 | 37.5 | 15.1 | 0.40 |
| Cu–Cr-2 | 0.005 M $CrO_4^{2-}$ | 94.64 | 3.83 | 1.53 | 56.6 | 20.3 | 0.36 |
| Cu–Cr-3 | 0.01 M $CrO_4^{2-}$ | 93.03 | 4.72 | 2.25 | 53.0 | 17.5 | 0.33 |
| Cu–Cr-4 | 0.05 M $CrO_4^{2-}$ | 91.61 | 5.57 | 2.82 | 60.2 | 15.4 | 0.26 |
| Cu–Cr-5 | 0.1 M $CrO_4^{2-}$ | 90.58 | 5.94 | 3.48 | 65.4 | 13.8 | 0.21 |
| Cu–Cr-6 | 0.3 M $CrO_4^{2-}$ | 89.50 | 6.25 | 4.25 | 63.2 | 10.8 | 0.17 |
| Cu–Cr-7 | 0.6 M $CrO_4^{2-}$ | 87.50 | 7.40 | 5.10 | 82.2 | 10.6 | 0.13 |

[a] Cu–Cr samples 1–7 were prepared by technique A using $Na_2CrO_4$ solutions with concentrations as shown; Cu–Cr samples 8 and 9 were prepared by technique B with addition of the quantities of 0.1 M $Cr(NO_3)_3$ solution as shown.

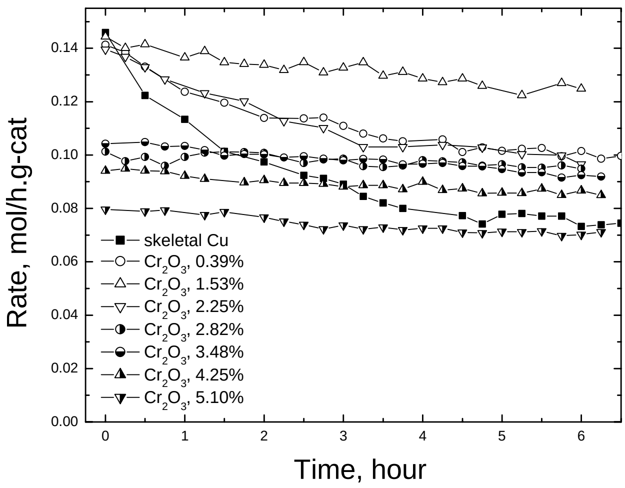

Fig. 1. Variation in the activity of un-promoted and chromia promoted catalysts with time-on-stream at 453 K.

The relationship between the specific initial activity (expressed as moles of methanol converted per square meter of copper per hour) and the chromia concentration is shown in Fig. 2. The addition around 2.0 wt.% of $Cr_2O_3$ decreased the initial specific activity to less than half that for the pure skeletal copper. Further increases in the amount of chromium oxide had an insignificant effect on specific initial activity. By contrast, the specific activity at 6 h on stream was independent of chromia content within the limits of the scatter. While there is good evidence to suggest that deactivation is associated with deposition of foulant in the form of polymerized formaldehyde [10], the exact reason for the variation in deactivation between catalysts is unclear. One possible explanation is that the leaching process creates a small percentage of copper sites that are especially active for hydrogenolysis, but are also easily blocked by deposited material, either foulant during reaction or chromia should this be present during preparation. In this situation one would expect chromia-containing samples to have a lower initial activity than pure skeletal copper, since fewer highly active sites will be present, but also as a consequence to exhibit less deposition of foulant, and hence deactivation with time-on-line. All catalysts would then tend to deactivate towards the same final specific activity determined by residual less active copper sites.

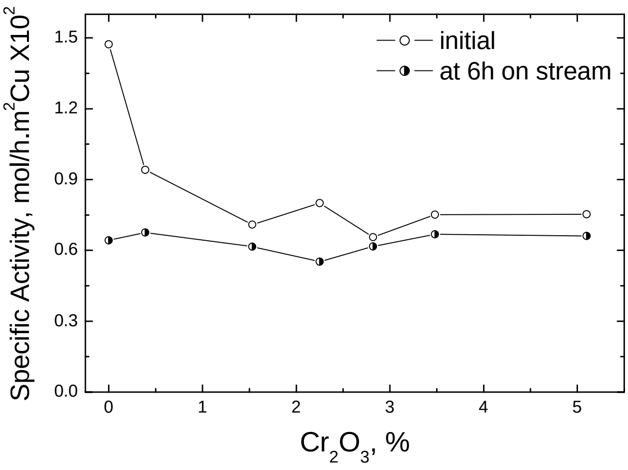

Fig. 2. Specific activity at 453 K as a function of $Cr_2O_3$ content for chromia promoted skeletal copper samples.

### 3.3. Deactivation and model considerations

In an earlier study of methyl formate hydrogenolysis over copper-based catalysts, Monti et al. [10] suggested that the deactivation process should be regarded as blocking of the surface, which eventually renders part of the copper surface inaccessible to the reactants. Formaldehyde is produced and is incorporated in a polymer chain attached and growing on the copper surface. It has been shown that highly dispersed copper is less affected by deactivation than pure coppers such as Raney® copper [8]. Recently Bryden and Garrett [23] studied the polymerization of formaldehyde on Cu and proposed that formaldehyde has a low activation barrier to polymerization and polymerization can be self-initiating by radical production. It was also found that formaldehyde adsorbed on clean Cu forms poly(oxymethylene) (POM) with differing chain lengths, the long (alpha) and the short (beta). Depolymerisation is easy when the chains are long but may become much harder when the chains are short [23]. In this study, the formaldehyde concentration will be low during the hydrogenolysis reaction and most likely short-chain polymer species are obtained from spontaneous polymerization of formaldehyde.

Previous studies showed that the deactivation for skeletal copper is due to deposition of polymers formed from adsorbed formaldehyde on the most active copper sites rather than those less active. The skeletal Cu–$Cr_2O_3$ catalysts have fewer of the high activity sites than unpromoted copper, hence the presence of $Cr_2O_3$ mitigates the fouling of skeletal copper. Furthermore, kinetics for deactivation over pure skeletal copper and chromia-promoted skeletal copper catalysts were carried out based on our experimental findings.

#### 3.3.1. Simple power-law equation

Normally the effects of deactivation on the rate of a single reaction can be modeled by introducing an activity function $a$ into the rate equation for the main reaction and a simple power-law equation (PLE) can be used. The activity function $a$ can be expressed as the rate of reaction on the deactivated catalyst divided by the rate on the fresh catalyst ($a = r_t/r_0$) and $\eta_d$ is the effectiveness factor which accounts for effects of pore diffusion resistance. The decrease in activity with time or deactivation rate is given by

$$-r_d = \frac{-da}{dt} = k_d(T) f(C) \eta_d a^d \tag{2}$$

In the case of hydrogenolysis of methyl formate to methanol reaction (Eq. (1)) over skeletal copper catalysts, the empirical power-law equation is expressed as the following:

$$-r = kC_{\mathrm{MF}}{}^{\alpha}C_{\mathrm{H_2}}^{\beta} \tag{3}$$

where $-r$ is the rate of disappearance of methyl formate based on unit mass of catalyst (mol/h g cat), $k$ the reaction rate constant (mol/h g cat kPa$^{-(\alpha+\beta)}$), $C_i$ the concentration of reactant for species $i$ (kPa), and $\alpha$, $\beta$ the concentration dependencies.

A study of hydrogenolysis reaction kinetics [19] has shown that the order with respect to methyl formate is very close to zero for both skeletal copper and copper chromite catalysts and that methanol has little effect on the rate of reaction. It is assumed that $f(C)$ is constant, and $\eta_{\mathrm{d}}$ has a value of unity because of the large pores in skeletal copper [17], hence Eq. (2) can be simplified to

$$-r_{\mathrm{d}} = \frac{-\mathrm{d}a}{\mathrm{d}t} = k_{\mathrm{d}}a^{d} \tag{4}$$

Because the deactivation is caused by fouling, it is suggested that the deactivation process can be considered to be one in which the reactant, methyl formate (A), produces two products, methanol (P) and fouling substance (F), and then the deactivation can be considered to be the parallel type (A $\rightarrow$ P; A $\rightarrow$ F$_{\downarrow}$). Integration of Eq. (4), assuming $d = 1$, 2 or 3 leads to

$$-\ln a = k_{\mathrm{d}}t \quad \text{(PLE first order)} \tag{5a}$$

$$\frac{1-a}{a} = k_{\mathrm{d}}t \quad \text{(PLE second order)} \tag{5b}$$

$$\frac{1-a^2}{2a^2} = k_{\mathrm{d}}t \quad \text{(PLE third order)} \tag{5c}$$

The data in Fig. 1 were modeled using Eqs. 5(a)–5(c) and the linear regression program in Excel. The fits calculated from the parameters obtained were poor for catalysts containing copper alone as shown in Fig. 3(a). The regression coefficient ($R^2$) improved as the order of deactivation increased in the order first, second and then third but clearly an order of 4 or more would be required to give good fit. Chromia-containing catalysts showed the same trend for the fit to improve with order (Table 2) but the differences between the models lessened for high chromia contents. This lack of difference is primarily a reflection of the higher stability of such catalyst so that the extent of deactivation over the time period employed is insufficient to enable discrimination.

Table 2
Deactivation rate constants calculated using first-, second- and third-order PLE models for the data in Fig. 1(a) and (b)

| Catalyst | First order | | Second order | | Third order | |
|---|---|---|---|---|---|---|
| | $k_{\mathrm{d}}$ | $R^2$ | $k_{\mathrm{d}}$ | $R^2$ | $k_{\mathrm{d}}$ | $R^2$ |
| Cu-A | 0.13 | 0.64 | 0.18 | 0.81 | 0.26 | 0.90 |
| Cu–Cr-1 | 0.065 | 0.80 | 0.077 | 0.86 | 0.091 | 0.90 |
| Cu–Cr-2 | 0.028 | 0.85 | 0.030 | 0.86 | 0.032 | 0.88 |
| Cu–Cr-3 | 0.069 | 0.89 | 0.080 | 0.92 | 0.095 | 0.94 |
| Cu–Cr-4 | 0.010 | 0.90 | 0.010 | 0.90 | 0.011 | 0.90 |
| Cu–Cr-5 | 0.019 | 0.98 | 0.020 | 0.98 | 0.021 | 0.97 |
| Cu–Cr-6 | 0.018 | 0.95 | 0.019 | 0.96 | 0.020 | 0.96 |
| Cu–Cr-7 | 0.023 | 0.92 | 0.024 | 0.93 | 0.026 | 0.93 |

### 3.3.2. Generalized power-law equation

The traditional power-law equations for deactivation are applicable only when the activity decays to zero. If a non-zero steady-state activity ($a_{\mathrm{s}}$) is reached, use of Eqs. 5(a)–5(c) will result in incorrect values for the deactivation order. Generalized power-law equations (GPLE) for catalyst deactivation were first suggested by Fuentes [24], whose treatment leads to a deactivation rate equation of the form

$$\frac{-\mathrm{d}a}{\mathrm{d}t} = k_{\mathrm{d}}\,f(C)(a-a_{\mathrm{s}})^{d} \tag{6}$$

The use of the GPLE treatment resulted in improved fit of the deactivation data at different temperatures compared with the PLE model assuming zero steady-state activity. Therefore a steady-state activity was assumed and analysis of deactivation data using Eq. (6) when $d = 1$ or 2 led to

$$\ln\frac{1-a_{\mathrm{s}}}{a-a_{\mathrm{s}}} = k_{\mathrm{d}}t \quad \text{(GPLE first order)} \tag{7a}$$

$$\frac{1}{a-a_{\mathrm{s}}} - \frac{1}{1-a_{\mathrm{s}}} = k_{\mathrm{d}}t \quad \text{(GPLE second order)} \tag{7b}$$

The data for all catalysts were fitted to these equations using the Solver routine in Excel and typical fits are shown in Fig. 4. Comparison of Fig. 4 with Fig. 3 shows that both GPLE models provide much better fits than do any of the three PLE models. The first-order GPLE model is marginally better than the second GPLE one on the basis of the regression coefficient and much better in the terms of the standard error for the corresponding deactivation parameters.

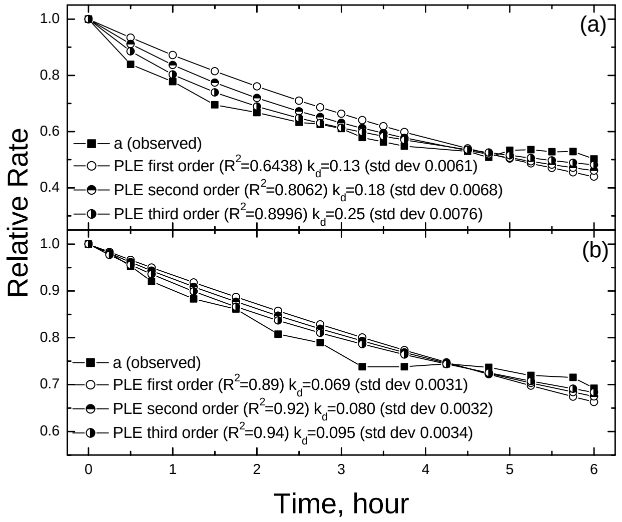

Fig. 3. Test of power-law deactivation models for (a) pure skeletal Cu and (b) skeletal Cu–$Cr_2O_3$ (1.53%) using data from Fig. 1.

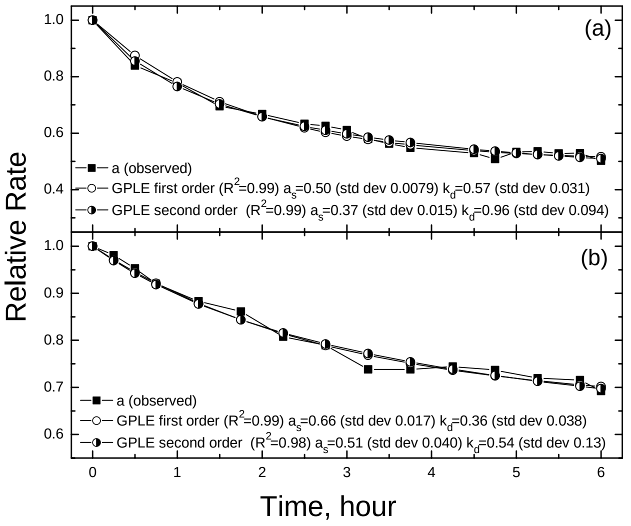

Fig. 4. Test of first- and second-order GPLE deactivation models for (a) pure skeletal Cu and (b) skeletal Cu–$Cr_2O_3$ (1.53%) using data from Fig. 1.

### 3.3.3. Deactivation kinetic parameters

Fig. 5 illustrates the influence of the different chromia concentration on the GPLE first-order deactivation constants, which were obtained from the data in Fig. 1. It can be seen that the $k_d$ value gradually decreases with the increased amounts of chromia deposited and that increased steady-state activities were achieved when chromia was present.

Several of the chromia-promoted skeletal copper samples containing <3.5% $Cr_2O_3$ were studied at different temperatures and plots of the calculated steady-state activities with chromia contents are shown in Fig. 6, from which it can be seen that the skeletal copper catalysts promoted with chromia exhibited improved steady-state activities when compared with pure skeletal copper at temperatures above 450 K. The best performance at all temperatures was found for 1.5 wt.% $Cr_2O_3$.

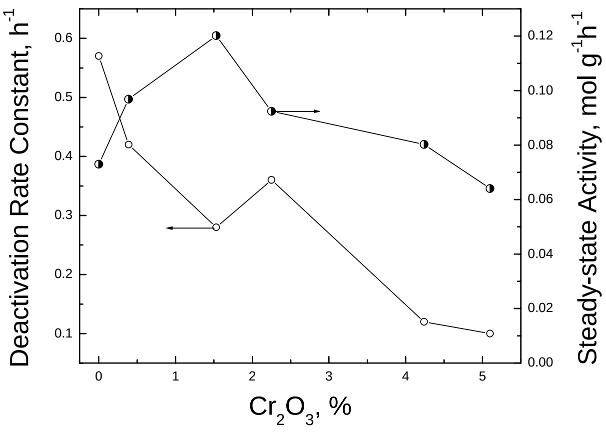

Fig. 5. Plots of deactivation rate constant and steady-state activity calculated using GPLE first-order model for the chromia-promoted skeletal copper samples at 453 K.

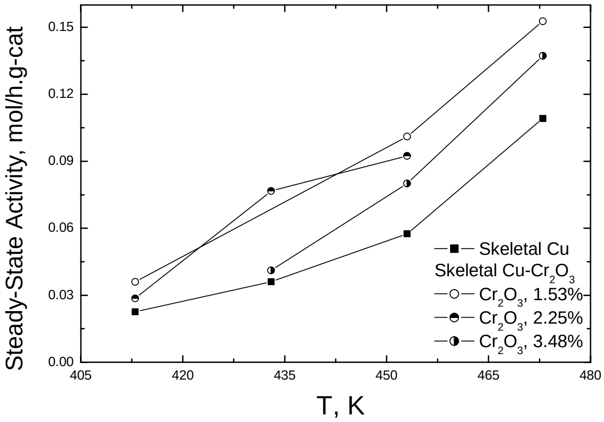

Fig. 6. Plots of the calculated steady-state activities for pure skeletal Cu and skeletal Cu–$Cr_2O_3$ catalysts at different temperatures.

## 4. Conclusions

Depositing chromia on skeletal copper reduced the deactivation caused by fouling with polymerized formaldehyde. The best improvement was achieved by depositing chromia in the range of 1.0–2.5% but higher chromia loadings decreased initial activity without further improving stability. The specific initial activity for methyl formate hydrogenolysis decreased with chromia loading up to around 1.5% and then remained stable at approximate half of the value for pure skeletal copper at higher loadings. It is suggested that the deactivation is due to deposition of the foulants on the most active sites rather than less active ones and that the skeletal Cu–$Cr_2O_3$ catalysts have fewer high activity sites than unpromoted Cu and that is the reason for $Cr_2O_3$ mitigating the fouling of skeletal copper. A GPLE first-order deactivation model, based on parallel deactivation and non-zero steady-state activity, fitted the deactivation phenomena. Skeletal copper promoted with 1.5% chromium oxide had the best steady-state activity at all temperatures studied.

## Acknowledgements

Financial support of an Australian Postgraduate Award (APA) for Xinwei Huang is gratefully acknowledged. We gratefully acknowledge the on-going support of the Australian Research Council.

## References

[1] T. Turek, D.L. Trimm, N.W. Cant, Catal. Rev. -Sci. Eng. 36 (1994) 645.
[2] D.S. Brands, E.K. Poels, T.A. Krieger, O.V. Makarova, C. Weber, S. Veer, A. Bliek, Catal. Lett. 36 (1996) 175.
[3] D.S. Brands, E.K. Poels, A. Bliek, Appl. Catal. A 184 (1999) 279.
[4] G.H. Xu, Y.C. Li, Z.H. Li, H.J. Wang, Ind. Eng. Chem. Res. 34 (1995) 2371.

[5] D.J. Thomas, Ph.D. Thesis, The University of New South Wales, Australia, 1990.
[6] J.W. Evans, N.W. Cant, D.L. Trimm, M.S. Wainwright, Appl. Catal. 6 (1983) 355.
[7] J.W. Evans, P. Casey, M.S. Wainwright, D.L. Trimm, N.W. Cant, Appl. Catal. 7 (1983) 31.
[8] D.M. Monti, M.S. Wainwright, D.L. Trimm, N.W. Cant, Ind. Eng. Chem. Prod. Res. Dev. 24 (1985) 397.
[9] J.W. Evans, M.S. Wainwright, N.W. Cant, D.L. Trimm, J. Catal. 88 (1984) 203.
[10] D.M. Monti, N.W. Cant, D.L. Trimm, M.S. Wainwright, J. Catal. 100 (1986) 17.
[11] M.A. Kohler, M.S. Wainwright, D.L. Trimm, N.W. Cant, Ind. Eng. Chem. Res. 26 (1987) 652.
[12] T. Turek, D.L. Trimm, D.St.C. Black, N.W. Cant, Appl. Catal. A 116 (1994) 137.
[13] N.I. Onuoha, M.S. Wainwright, Chem. Eng. Commun. 29 (1984) 1.
[14] D.J. Thomas, D.L. Trimm, M.S. Wainwright, N.W. Cant, Chem. Eng. Process. 31 (1992) 241.
[15] D.J. Thomas, M.S. Stammbach, N.W. Cant, M.S. Wainwright, D.L. Trimm, Ind. Eng. Chem. Res. 29 (1990) 204.
[16] L. Ma, M.S. Wainwright, in: D. Morrell (Ed.), Catalysis of Organic Reactions-Chemical Industries, Marcel Dekker, Inc., New York, 2002, p. 225.
[17] L. Ma, M.S. Wainwright, Appl. Catal. A 187 (1999) 89.
[18] J.W. Evans, M.S. Wainwright, A. Bridgewater, D.J. Young, Appl. Catal. 7 (1983) 75.
[19] X. Huang, N.W. Cant, J.W. Evans, M.S. Wainwright, Catal. Today 93–95 (2004) 113.
[20] L. Ma, A.J. Smith, T. Tran, M.S. Wainwright, Chem. Eng. Process. 40 (2001) 59.
[21] A.J. Smith, L. Ma, T. Tran, M.S. Wainwright, J. Appl. Electrochem. 30 (2000) 1097.
[22] K.M. Kim, H.C. Woo, M. Cheong, J.C. Kim, K.H. Lee, J.S. Lee, Y.G. Kim, Appl. Catal. A 83 (1992) 15.
[23] T.R. Bryden, S.J. Garrett, Langmuir 17 (2001) 5850.
[24] G.A. Fuentes, Appl. Catal. 15 (1985) 33.